Available online at www.sciencedirect.com

ScienceDirect

Energy Procedia 6 (2011) 777–785

Energy Procedia

MEDGREEN 2011-LB

Unsteady Loads Evaluation for a Wind Turbine Rotor using free wake method

Said CHKIR

Faculté de Génie Mecanique et Electrique, Damascus university,
said.chkir@gmail.com
P.O.Box 615 Damascus,Syria

Abstract

This paper presents a method for calculating the flow around a wind turbine rotor. The real flow is replaced by a free stream past a vortex model of the rotor. This model consists of lifting vortex lines which replace the blades and a trailing free vorticity. The vorticity shed from the blade is concentrated in two vortices issued from tip and root. To compute the unsteady forces exerted on the rotor, a free wake method is used. This method consists of a Lagrangian representation of the flow field. The evolution of the wake is obtained by tracking the markers representing the vortices issued from the blade tips and roots. To solve the wake governing equation and to obtain the marker positions, a time-marching method is applied and the solution is obtained by a second order predictor-corrector scheme. To validate the proposed method a comparison is made with experimental data obtained in the case of a model of wind turbine where the flow field immediately behind the rotor is measured by means of PIV. It is shown that the numerical simulation captures correctly the near wake development. The comparison shows satisfactory accuracy for the velocity field downstream of the rotor.

1876–6102 © 2011 Published by Elsevier Ltd. Open access under CC BY-NC-ND license.
doi:10.1016/j.egypro.2011.05.088

"Keywords: Wind turbine/ Unsteady aerodynamics/ Vortex/ Wake/PIV ;"

1. Introduction

In the last few decades, wind energy has become the leading contender among the renewable sources of energy. Wind turbines are playing a significantly increasing role in the generation of electrical power that can then be used in various applications.

Wind turbines operate in a complex unsteady flow environment composed of various effects such as atmospheric turbulence, ground boundary layer effects, directional and spatial variations in wind shear and the effects of the tower shadow. The estimation of the velocity field and local angle of attack of the blade's profiles could be the key to predict the aerodynamic loads on the rotor and the power generated by wind turbine. Improving the capability of the numerical tools to predict the aerodynamic and mechanical forces applied to the rotor, is one of the most important factors to optimize their design, operating and maintenance costs and to verify their reliability.

Methods concerned with the prediction of the aerodynamic loading and performance of wind turbines assume that the fluid is inviscid and incompressible. In the most common method, the Blade Element Momentum Theory (BEM) methods [1], the blade is divided into several segments with cylindrical surfaces and the calculation is performed segment by segment. All blade elements are assumed to operate independently of each other. Accordingly, if lift and drag forces are determined for each element, it will be then possible to evaluate the rotor characteristics. In the present free wake method, the airfoil relative velocity is corrected by the induced velocity. The axial and tangential induced velocities are calculated for each section using momentum theorem. The BEM methods are simple to use, require little computer time and provide accurate results, however, it contains invalid assumptions which are overcome in practice by empirical adjustments.

In recent years the resolution of the Navier-Stokes equations [2] has become a preferred method in all the domains of fluid mechanics. The advantages of this method are well known, especially the possibility of obtaining a solution in very complex flows cases. Despite the good results in most cases, these methods need huge computational costs and large memory requirements that delayed their practical use for many problems, including helicopter and wind turbine applications.

The vortex methods are potential methods based on the replacement of the real flow through the rotor by an inviscid fluid flow through an equivalent vortex system. This system consists of blade attached vortices and free vortices trailed into the wake. According to the representation manner of the vortex wake, there are two different approaches: prescribed wake and free wake. The prescribed wake method assumes that the wake shape is known, either through testing, or from an approached calculation [3]. In unsteady conditions and if the induced velocity is important, the wake shape varies in time and the prescribed wake method is therefore not applicable. In this case, the free wake method is preferred and we will describe its principles in the following.

Nomenclature

α	Lamb-Oseen constant
δ	Effective eddy-viscosity coefficient
$\vec{r}$	Position vector of vortex control point
t_0	Initial position at time = 0

ψ_w	Vortex wake age
ψ_b	Azimuthal angle
V_∞	Free-stream velocity vector
Γ	Vortex strength, Circulation (m/s)
ρ	Density of air
α	Lamb-Oseen constant
N	Number of rotor blades
W	Wind relative velocity
V_{ind}	Induced velocity vector
r_t	Blade tip radius, (m)
r_h	Blade root radius, (m)
t_0	Initial position at time = 0
$d\ s$	Element of the vortex.
r_0	Initial viscous core radius
r_c	Viscous core radius
a_1	Turbulent viscosity constant
Re_v	Vortex Reynolds number
Ω	Rotational speed of the rotor (rad/s)
ϕ	Flow angle
v_i	Self-induced velocity at point i
Δs	Finite length vortex segments left (right) of the control point
C_L	Lift coefficient
C_D	Drag coefficient
F	Blade forces
Q	Rotor torque
P	Power

2. Methodology

The free wake method is originally used in the analysis of helicopter rotors [4]. These models created for helicopter rotors have been later adapted for the calculation of wind turbines rotors [5]. In this vortex method, the real flow is replaced by a inviscid fluid flow through an equivalent vortex system.

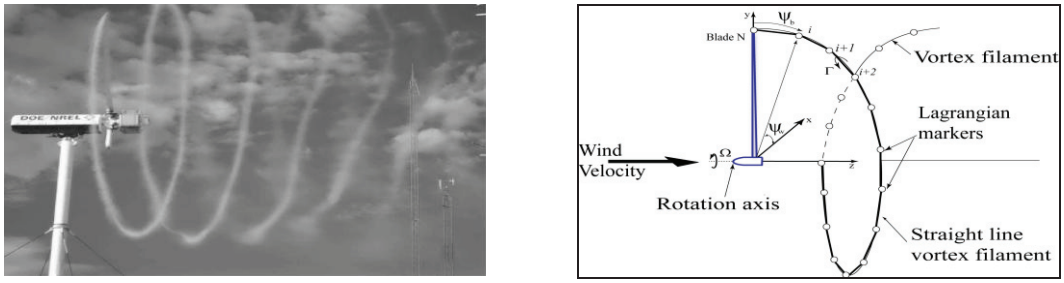

Figure 1. (a) Smoke flow visualization of the wind turbine wake (source: NREL) ; (b) Representation of the rotor wake

This system consists of vortex attached to each blade (exerting on the fluid the same forces as those applied by the blades) and a wake consisting of a strong tip-vortex emanating from each blade tip and root (Figure.1 (a) and (b)). In this work, a Lagrangian description of the flow is used. Lagrangian markers are distributed along each tip-vortex filament (Figure.1 (b)). Thus, tip-vortex filaments are discretized and the markers are linked together, usually with straight line segments. This allows the induced velocity to be determinated using the Biot-Savart law:

$$d\vec{V}_{ind} = \frac{\Gamma}{4\pi}\frac{d\vec{s}\times\vec{r}}{|\vec{r}|^3}. \quad (1)$$

The spatio-temporal evolution of the markers in the rotor wake can be derived from Helmholtz's law (vorticity transport theorem) buy assuming that for each point in the flow the local vorticity is convected by the local velocity. The fundamental equation describing the transport of the filament is:

$$\frac{d\vec{r}}{dt} = \vec{V}. \quad (2)$$

Where $\vec{r}$ the position vector that can be represented using a function of two variables, which represent the spatio-temporal evolution of the Lagrangian markers position:

$$\vec{r} = \vec{r}(\psi_w, \psi_b). \quad (3)$$

In equation (3), ψ_w is the azimuth angle (wake age) corresponding to the vortex that was trailed from the blade when it was at an azimuth angle ψ_b.

Using these two angular variables and a constant angular velocity Ω of the wind turbine, the position vector $\vec{r}$ of a wake element can be expressed as a function of the azimuthal blade position ψ_b and the age of the filament ψ_w relative to the blade when it was introduced into the wake. Equation (2) can, therefore, be written in the non-rotating, hub-fixed coordinate system as:

$$\frac{\partial\vec{r}}{\partial\psi_w} + \frac{\partial\vec{r}}{\partial\psi_b} = \frac{1}{\Omega}\vec{V}. \quad (4)$$

where the velocity $\vec{V}$ has contributions from the free stream and the highly nonlinear self and mutually induced velocities corresponding to the vortex wake structure. Note that equation (4) is a first-order, partial differential equation. The homogeneous portion of this equation is hyperbolic, However, the right-hand side, which includes the induced velocity by the attached and the free vortex, is highly nonlinear.

The complexity of the solution of equation (4) arises from the nonlinearity and the singularity of the vortex filaments. To simplify the calculation, the blade surface must be replaced by a vortex line with a constant circulation. This simplification can be justified in the case of high lengthening blades, as observed in wind turbines. A numerical solution of equation (4) may be made by using a second order predictor-corrector scheme to improve the accuracy and the stability of the numerical algorithm. The discretization of equation (4) is presented in (Figure 2 (a)) using a five-point central differencing scheme.

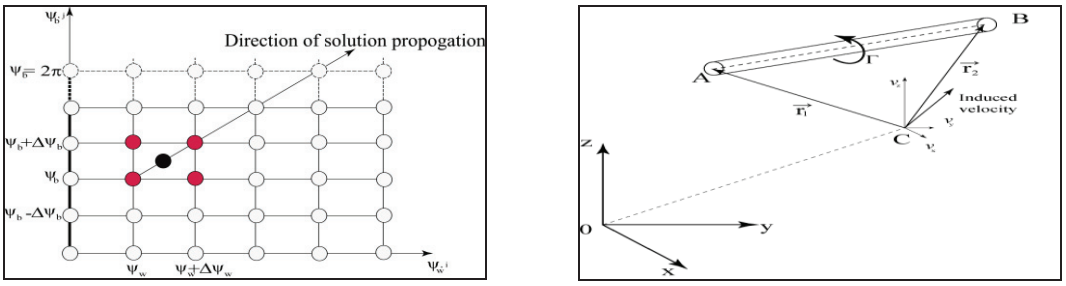

Figure 2. (a)Five-point central differencing scheme,(b) Straight line vortex filament induced velocity calculation at point C.

The predictor step is used to obtain an intermediate solution at the new time step to enable the induced velocity calculation $\vec{V}^{n}_{j+\frac{1}{2}}$ to proceed by using Biot-Savart law as:

$$\tilde{\vec{r}}_{j+1} = \vec{r}^{\,n}_{j} + \frac{2}{\Omega}\left(\frac{\Delta\psi_w.\Delta\psi_b}{\Delta\psi_w + \Delta\psi_b}\right)\vec{V}^{n}_{j+\frac{1}{2}} \tag{5}$$

The corrector step is obtained by averaging the induced velocity $\tilde{\vec{V}}_{j+\frac{1}{2}}$ from the previous at (n-1)th step with $\vec{V}_{j+\frac{1}{2}}$ at (n)th as:

$$\vec{V}^{\,n+\frac{1}{2}}_{j+\frac{1}{2}} = \frac{1}{2}\left(\vec{V}^{n}_{j+\frac{1}{2}} + \tilde{\vec{V}}_{j+\frac{1}{2}}\right). \tag{6}$$

Then, this value is used with the obtained value of (5) in the corrector step as:

$$\tilde{\vec{r}}^{\,n+1}_{j+1} = \vec{r}^{\,n}_{j} + \frac{2}{\Omega}\left(\frac{\Delta\psi_w\,\Delta\psi_b}{\Delta\psi_w + \Delta\psi_b}\right)V^{\,n+\frac{1}{2}}_{j+\frac{1}{2}}. \tag{7}$$

The local air velocity relative to the rotor blade consists of the free-stream velocity and the wake induced velocities as:

$$\vec{V} = \vec{V}_{\infty} + \vec{V}_{ind}. \tag{8}$$

The wake induced velocity is evaluated by the application of the Biot-Savart law (1) as an integral along the complete length of each vortex wake filament. For a vortex segment of length AB (Figure.2 (b)), the induced velocity at a point C can be written as:

$$d\vec{V}_{ind\,C} = \frac{\Gamma}{4\pi}(\vec{r}_1 \times \vec{r}_2)\left(\frac{1}{|\vec{r}_1|\cdot|\vec{r}_2| + \vec{r}_1\cdot\vec{r}_2}\right)\left(\frac{|\vec{r}_1| + |\vec{r}_2|}{|\vec{r}_1|\cdot|\vec{r}_2|}\right). \tag{9}$$

The vortex straight segment representation of the tip-vortex can give rise to a number of errors near the control point. Because a straight vortex of any length cannot induce a velocity on itself, the contribution of vortex straight-segment left and right of the control point is zero, so a curvature correction should be applied [6]. The correction is made only to the segments which begin or end at the control point, where the self-induced velocity is needed. The viscous core radius r_c is used like a lower limit, arising from the logarithmic singularity in the integrand for any curved vortex (Figure.3). The self-induced velocity can be calculated through the application of the Biot-Savart law along a curved vortex filament. In order to avoid a logarithmic singularity at the control point, a logarithmic formula proposed by Hama [7] is used:

$$\vec{v}_i = -\frac{\Gamma(\frac{\partial \vec{r}}{\partial s}) \times (\frac{\partial^2 \vec{r}}{\partial s^2})}{4\pi \left| \frac{\partial \vec{r}}{\partial s} \right|^3} \ln r_c \,. \tag{10}$$

The value of r_c, is in the range [0.01, 0.03], it represents the core radius of the viscous vortex and allows to take into account his actual structure.

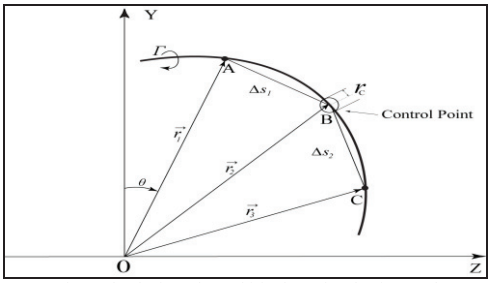

Figure 3. Strategy for calculating the self-induced velocity at the control point B

Because of the viscous effects, the core radius of the tip vortices does not remain constant and increases as its progress downstream of the flow. Leishman and Bhagwat [8] suggested an empirical approach to calculate the growth of the viscous core radius:

$$r_c(\psi_w) = \sqrt{r_0^2 + \frac{4\alpha\delta\nu\psi_w}{\Omega}} \,. \tag{11}$$

Here, the eddy-viscosity coefficients δ takes into account the diffusion rate of the tip vortex, which must be a function of the Reynolds number as:

$$\delta = 1 + a_1 \,\mathrm{Re}_v \,. \tag{12}$$

The experimental values of α and a_1 are obtained by [9]. It may be noted also that the circulation Γ decreases along the vortex filament, and causes significant induced velocity changes. Indeed, this circulation reduction can be taken into account from experimental data.

At each time step, a new vortex detached from the blade tip and each element of the wake vortex moves in the local velocity direction. Firstly we get this displacement and the wake form. Then, we calculate the induced velocity by the free wake vortices and blade attached vortices, over the entire blade span. These induced velocities allow obtaining the relative velocity distribution and the angles of attack along the blade. Finally at each time step and by means of the Kutta-Joukowski lift theorem we obtain the circulation. For the steady case, we can calculate The aerodynamic efforts exerted on a wind turbine rotor (the calculations of blade forces *F*, rotor torque *Q*, and the power *P)* by using the formula:

$$F = \int_{r_r}^{r_t} \frac{1}{2} \rho N c W^2 (C_L \cos\phi + C_D \sin\phi) dr \tag{13}$$

$$Q = \int_{r_r}^{r_t} \frac{1}{2} \rho NcW^2 (C_L \sin\phi - C_D \cos\phi) r dr \tag{14}$$

$$P = \int_{r_r}^{r_t} \frac{1}{2} \rho NcW^2 (C_L \sin\phi - C_D \cos\phi) r \Omega dr \tag{15}$$

If the blades circulation does not vary any more, we stop the calculation, and then the aerodynamic characteristics of the wind turbine can be evaluated by (13), (14) and (15).

3. Results and Discussion

The calculation results show the robustness of the predictor-corrector scheme proposed. Here, we present only the wake calculation results witch compared with laboratory measurements made with PIV. The study focused on areas where wake modeling requires attention; in particular, the strength and geometry of trailing tip vortex, vital for the prediction of fluid loading on the rotor blades.

The PIV experiments reported in the present paper were conducted at the ENSAM-Paris wind tunnel using a modified commercial wind turbine Rutland 503. This horizontal axis wind turbine has a three blades rotor with a diameter of 0.5 m and a hub diameter of 0.135 m. The blades are tapered and untwisted. They have a pitch angle of 10° and a chord of 0.045 m at tip and 0,065 m at root. The rotational speed is 1000 rpm with a free-stream velocity of 9.3 m/s. Hence, the tip to speed ratio is equal to 3, which is lower than the case of market wind turbines. The wind turbine is mounted on a support tube of 0.037 m of diameter ensuring a sufficient height in order to allow the lasers fixed above the transparent roof to illuminate the explored plane with an adequate intensity. The PIV technique is applied to obtain the velocity in the wake downstream of the turbine rotor.

In order to reduce the blade airfoil characteristics influence on the calculation an imposed circulation is used. The circulation used here comes from the test results realized at the ENSAM-Paris wind tunnel [10].

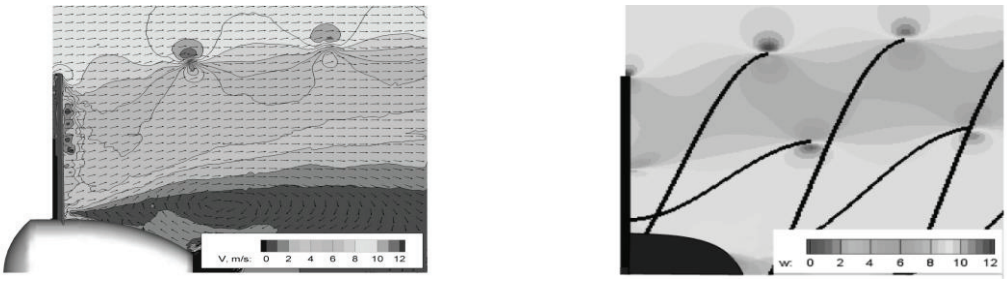

Figure 4. (a)Downstream axial velocity field, Rutland 503 wind turbine (m/s),(b) Side view of the Rutland 503 near wake calculated by the present free-wake method

The wake vortex shape is presented in (Figure.5), it generally fits the experimental wake shown in (Figure.4(a)). The axial velocity field in the rotor plane and in the azimuth plan is presented in (Figure.6). It may be noted, outside the wake, the wind is accelerated by the axial component of the induced velocity of all the vortices. However, in the wake, the induced velocity is slowing the flow. Accordingly, downstream of the turbine the wake diameter is increases as the distance from the rotor increases. After some distance, the diameter remains constant in the simulation as in the experiment.

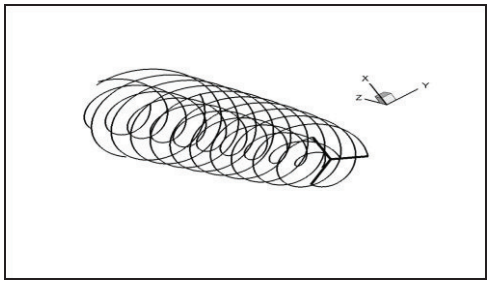

Figure 5. Downstream wake shape calculated by the present free wake method, Rutland 503 wind turbine

In the experiment (Figure. 4(a)), we can see that there is a vortex area behind the hub not represented in the simulation. In fact, in the case of industrial turbines, the hub is much smaller and this stall area and recirculation does not exist.

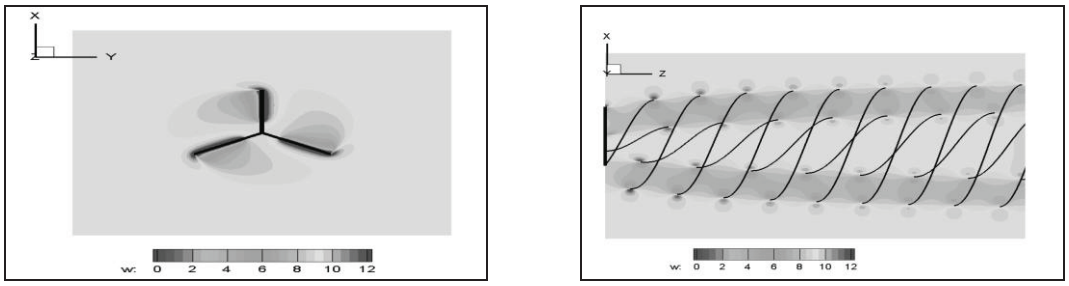

Figure 6. (a)Face view of the wake calculated by the present free-wake method, axial velocity (m/s) (b)Side view of the wake calculated by the present free-wake method

4. Conclusions

This paper has reviewed the theoretical basis and numerical implementation of one class of a free wake method, which was set up to calculate the flow downstream of a horizontal-axis wind turbine.
In this method, the rotor wake is discretized into vortex filaments defined by a series of Lagrangian markers. The governing equation for this free-wake problem is reduced to a system of first-order, partial differential equations that describe the convection of these markers through the flow.
Unlike the wake of the prescribed method, we calculate explicitly the tip vortex trajectory. The calculation results show that the wake has a helical form. The vortex issued from tip and root of each blade are not located on a cylindrical surface, as suggested by the linear vortex theory. They move outward by increasing the diameter of the vortex tube. A validation study for the prediction of the wake geometry behind a three-bladed wind turbine using a free-wake was performed for axial flow conditions, and was validated against idealized laboratory experiments using the PIV technique. The comparison reveals that accurate results can be obtained, for the operating conditions considered, with substantial savings of computer time.
The value of this approach in the future relies in that it will allow the evaluation of unsteady loads exerted on a wind turbine.

References

[1] Sørensen, JN., Mikkelsen, R, On the validity of the blade element momentum method, *Proceedings of the EWEC, Kopenhagen.* ., 2001

[2] Sørensen, JN., Michelsen, J., and Schreck, S, Navier-Stokes predictions of the NREL phase VI rotor in the NASA Ames 80x120 ft wind tunnel, *Wind Energy*., 2002, pp **151-169**

[3] Leishman, G, Challenges in modeling the unsteady aerodynamics of wind turbines, *Wind Energy*, 2002, 5(2-3):**85-132**

[4] Leishman, G., Principles of helicopter aerodynamics, *Cambridge Aero. Series*, 2000.

[5] Afjeh, A, Keith ,T., A Simplified Free Wake Method for Horizontal-Axis Wind Turbine Performance Prediction, *Journal of fluid engineering* , 1986 ,vol. 108 pp **400-406**.

[6] Wood, DH., Generic vortex modeling for horizontal-axis wind turbine, *Journal of fluid engineering*, 2002, 26(2), pp. **71-84**

[7] Hama, F., Progressive Deformation of a Curved Vortex by Its Own Induction, *Physics of fluids Journal*, , 1962 pp **1156-1162**

[8] Leishman, G., Bhagwat, M., Correlation of Helicopter Tip Vortex Measurement, *AIAA Journal*, 2000, Vol. 38, No 2, pp.301-308.

[9]Ramasamy, M., Leishman, G., Interdependence of Diffusion and Straining of Helicopter Blade Tip Vortices, *Journal of Aircraft*, 2004, 41(5):**1014-1024**

[10] Dobrev,I., Maallouf, B., Troldborg N., Massouh, F., Investigation of the Wind Turbine Vortex Structure, *14th Int Symp on App. of Laser Tech. to Fluid Mech*., 2008, Lisbon